

# Metallographic investigations of the heat-affected zone II/parent metal interface cracking in 18Ni maraging steel welded structures

P. RAMESH NARAYANAN, K. SREEKUMAR, A. NATARAJAN, P. P. SINHA  
*Materials and Metallurgy Group, Vikram Sarabhai Space Centre, Trivandrum 695 022, India*

During the fabrication of a large diameter pressure vessel out of 18Ni maraging steel by manual TIG welding, microcracks were noticed at the heat-affected zone (HAZ)/parent metal interface. The location of these cracks was very different from those reported at the fusion zone/HAZ I interface due to "constitutional liquation". Extensive optical metallography, scanning electron microscopy and energy dispersive X-ray analyses were carried out to identify the cause for the occurrence of these cracks. It is inferred from the experimental results that the microsegregation of titanium and nickel due to repeated thermal cycling during multipass welding led to the formation of TiC/Ti(CN) and stable austenite film on the grain boundaries. Under severe thermal stresses developed during welding, microvoids generated at the interface of TiC/Ti(CN) inclusions and austenite and further propagated intergranularly due to the premature failure of the austenite films.

## 1. Introduction

The 18Ni maraging steels are easily weldable over a wide range of thicknesses. Microstructurally they have well-defined welded structure, coarse-grained fusion zone, light etched heat-affected zone (HAZ I) and dark etched heat-affected zone (HAZ II). A weld efficiency of 95% to 100% is easily achieved in these steels after simple ageing heat treatment at 753 K. However, occasionally cracks in HAZ have been observed during fabrication near the terminal crater immediately adjacent to the fusion line. Previous investigators [1-3] have concluded that these cracks were formed due to "constitutional liquation" arising out of melting of some constituents much below the bulk solidus at the grain boundaries. The resultant grain-boundary films crack under severe thermal stresses generated in the fusion and heat-affected zones. The presence of cracks in the aerospace structural components made out of ultra-high-strength steels is highly undesirable from the fracture mechanics point of view. During the fabrication of a 3000 mm diameter pressure vessel out of 8.00 mm thick maraging steel plate by manual TIG welding in five passes, presence of fine cracks in the vicinity of HAZ II/parent metal interface were detected by dye penetrant and ultrasonic testing. The location of these cracks is schematically shown in Fig. 1. It is seen that these locations are much different from the often reported crack generation at the fusion zone/HAZ I interface in maraging steel weldments due to the phenomenon of "constitutional liquation". Pepe and Savage [1] demonstrated that a minimal temperature of 1590 K is required for the constitutional liquation to occur in this type of steel. Microstructurally,

materials exposed to such a high temperature would show excessive grain growth which is seen only near the fusion zone and not at the HAZ II/parent metal interface. These observations altogether preclude the possibility of a crack being generated due to constitutional liquation in the present case. Therefore, it was considered interesting to undertake a detailed microstructural analysis to establish the cause for the microcrack generation in areas far away from the fusion line. This paper reports the experimental findings and the conclusions drawn from this study to identify the mechanism of cracking at the HAZ II/parent metal interface.

## 2. Materials and experimental procedure

### 2.1. Materials

The steel used for the fabrication of the pressure vessel was melted in a vacuum melting furnace and subsequently refined by vacuum arc remelting. The nominal compositions of the steel and the filler wire used for welding are given in Table I.

### 2.2. Microstructural observations

Metallographic observations were carried out using optical microscope (OM), scanning electron microscope (SEM) and energy dispersive X-ray analysis (EDAX). The samples for microscopic observations were prepared by conventional methods and etched with an aqueous solution of 10% ammonium persulphate. The grain size in the different zones could be estimated on etching the above specimens with 10% Nital. The SEM and EDAX analyses were conducted at various locations near the origin and the end of the

TABLE I Chemical composition of the plates and filler wire

| Material    | Composition (wt %) |         |       |       |      |      |      |                |                |                |
|-------------|--------------------|---------|-------|-------|------|------|------|----------------|----------------|----------------|
|             | C                  | S and P | Ni    | Co    | Mo   | Ti   | Al   | O <sub>2</sub> | N <sub>2</sub> | H <sub>2</sub> |
| Plate       | 0.005              | 0.005   | 18.50 | 7.50  | 4.80 | 0.45 | 0.10 | 0.0017         | 0.002          | 0.003          |
| Filler wire | 0.006              | 0.005   | 18.14 | 11.85 | 2.54 | 0.16 | 0.46 | 0.003          | 0.003          | 0.0002         |

cracks, to study variations in the microstructures and the chemical homogeneity.

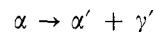
### 3. Results

Fig. 2 shows the gross microstructural features of the weldment and the HAZ. A typical micrograph at the crack-initiating regions is given in Fig. 3. It is seen that the crack initiated at the cuboidal/angular inclusions present at the grain boundaries and further propagated intergranularly from the HAZ II to the parent metal. The microstructural variations in the areas adjacent to the cracks, as revealed by SEM, are presented in Figs 4 and 5. The high-resolution micrograph (Fig. 5) clearly indicates the presence of white etched thin austenitic films along the martensitic laths and prior austenitic grain boundaries. However, the microstructures away from the cracks are devoid of any such film (Fig. 6). A typical energy dispersive spectrum on the inclusion is shown in Fig. 7. Table II presents the chemical composition of the areas nearer to and away from the crack end obtained by Tracor Northern X-ray analyser using the spot mode. It is evident that there exists high nickel (20 to 22 wt %) and high titanium (0.5 to 0.9 wt %) concentration regions near the origin of the cracks. The effect of chemical inhomogeneity on the hardness were estimated by measuring microhardness in aged conditions. Fig. 8 shows typical microhardness indentations near the grain boundaries having austenite films (marked a) and on the matrix (marked b). The microhardness values corresponding to a and b are found to be 180 to 200 and 550 to 560 VPN, respectively.

### 4. Discussion

It has been observed by a number of workers [4, 5] that, for cracks to generate in the HAZ during welding, the presence of both mechanical stresses and

weaker metallurgical constituents are essential. Along with the factors contributing to the mechanical stresses, such as constraints in the form of rigid fixturing, severe shrinkage stresses also are invariably present. These, and the metallurgical conditions resulting from the material chemistry and complex liquid  $\rightleftharpoons$  solid and solid  $\rightleftharpoons$  solid reactions due to rapid heating and cooling cycles involved during multipass welding, primarily control the quality of the welds. Optical micrographs (Fig. 2) of the welded and HAZ I regions did not show any evidence of microsegregation and conform to typical microstructures of 18 Ni maraging steel in the as-welded condition [6]. However, the presence of a thin austenitic film at grain boundaries (Fig. 5) and also the concentration of nickel and titanium as evidenced by the EDAX analysis (Table II) near the cracked region, indicate that the zone has undergone repeated heating and cooling cycle in the two-phase region of the iron-rich side of the Fe-Ni phase diagram during the multipass welding. A diffusion-controlled decomposition of martensite followed according to



where  $\alpha'$  is the alloy-depleted martensite, and  $\gamma'$  the alloy-rich stable austenite which does not transform to martensite during subsequent cooling. The degradation of the aged hardness adjacent to the origin of the crack is attributed to the presence of austenitic film and reduction in the titanium content in the area. Similar observations on the effect of austenite present on welded and heat-affected zones have also been reported by other investigators [3, 7]. The grain-boundary inclusions, analysed as titanium-rich phases by EDAX, were identified as TiC or Ti(CN) based on their morphology and colour, following the approach of Boniszewski and Boniszewski [8] and Psioda [9].

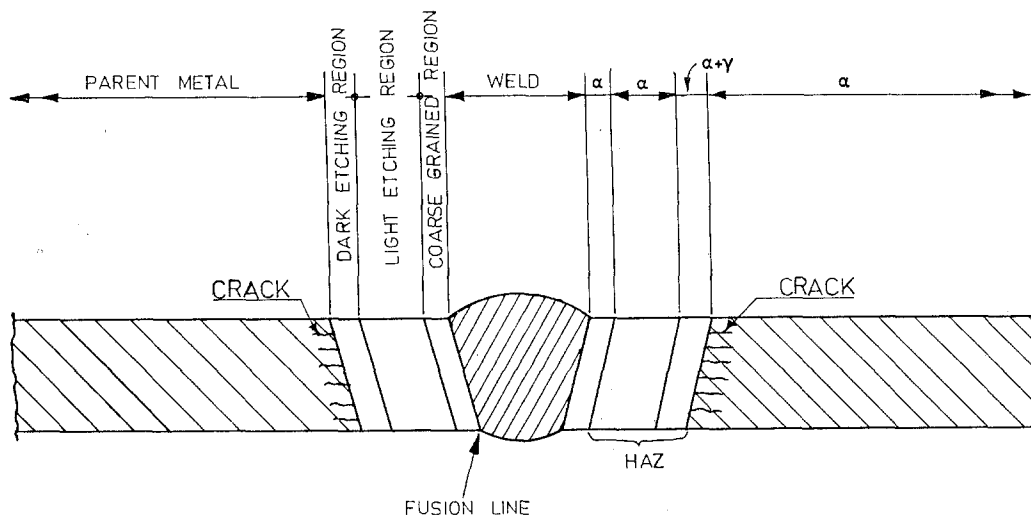


Figure 1 Schematic diagram showing the weld zone.

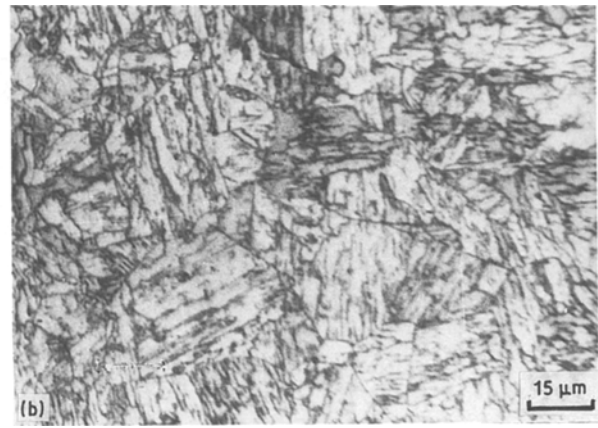
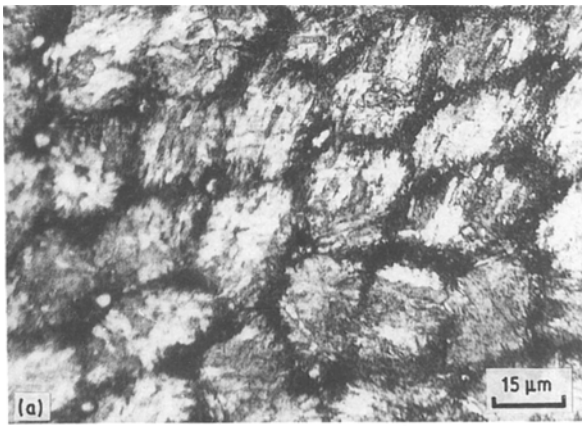


Figure 2 Microstructural features of (a) weldment, (b) light etched HAZ I and (c) dark etched HAZ II.

The formation of these carbides/carbonitrides was further attributed to the microsegregation of titanium at the grain boundary. Thus the experimental evidence clearly establishes that the grain-boundary segregation of titanium and nickel at the HAZ II/parent metal interface resulted in the formation of TiC/Ti(CN) inclusions and a stable austenitic film. In the presence of these adverse microstructural conditions, it is easy to hypothesize that the severe thermomechanical stresses generated during welding caused the formation of microvoids at the interfaces of TiC/Ti(CN) particles and austenitic film. Once these voids are nucleated at the grain boundaries, they are further propagated intergranularly due to the premature failure of the austenitic film. This is in accordance with Tettleman [10] who pointed out that when a softer phase is present in a harder matrix, the softer phase will reach the critical strain for fracture at an earlier stage, on loading. Consequently, this would lead to the generation of a series of microcracks even in a harder martensitic matrix.

## 5. Conclusions

The mechanism of HAZ II/parent metal cracking in maraging steel weldments is outlined based on extensive metallographic investigations. The following conclusions were drawn.

1. Repeated thermal cycling in the two-phase regions

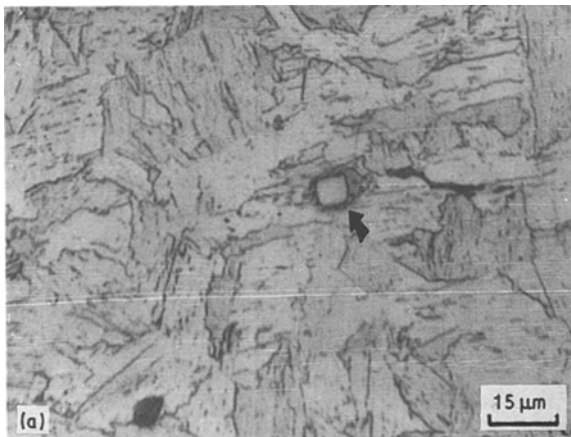


Figure 3 Microstructure at HAZ II/parent metal interface showing (a) crack initiation at a cuboidal inclusion, and (b) crack initiation at an angular inclusion and propagation along the grain boundaries towards parent metal.

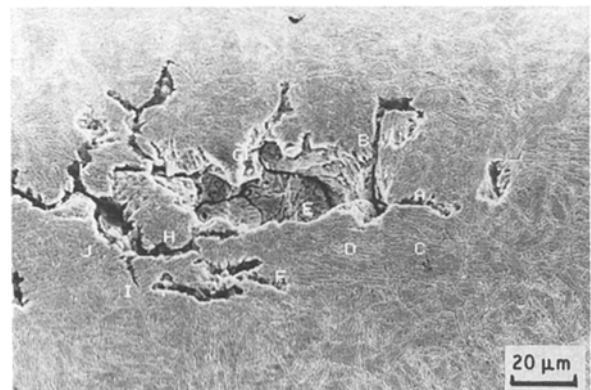


Figure 4 Scanning electron micrograph showing the topographical features of crack and identifying areas for EDAX and microstructural analysis.

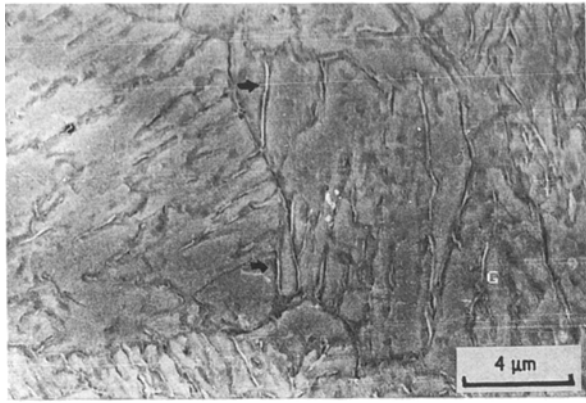


Figure 5 Scanning electron micrograph revealing the presence of a thin austenitic film along martensitic lath and prior austenitic grain boundaries corresponding to area (d) in Fig. 4.

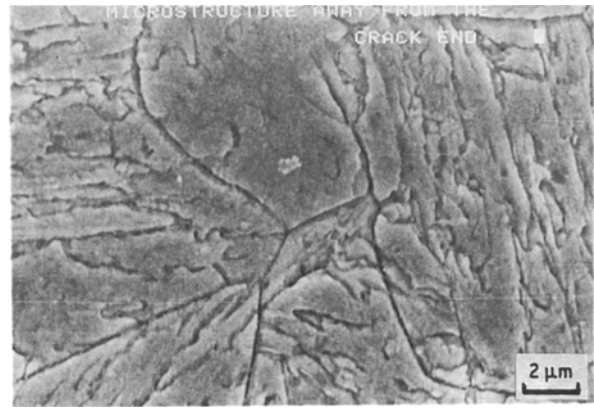


Figure 6 Microstructure (SEM) of the area away from the crack which does not show the presence of any austenitic film.

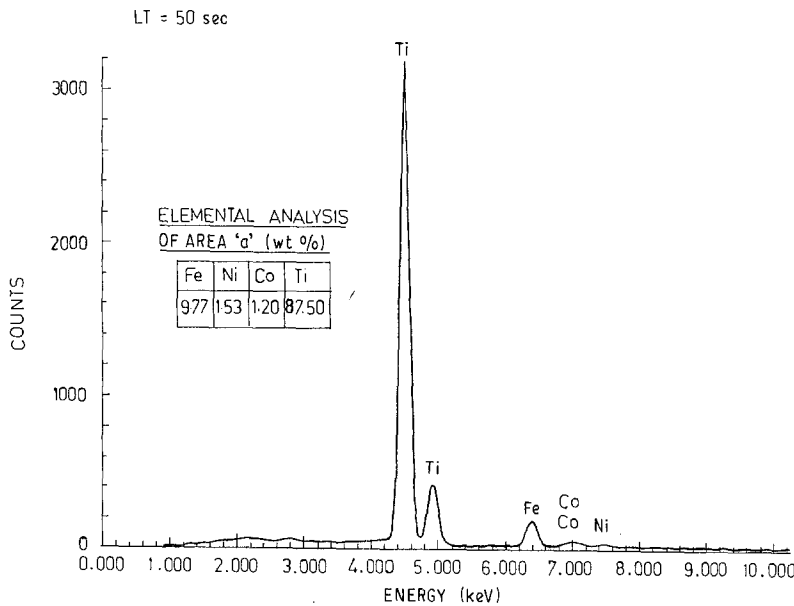


Figure 7 Typical energy dispersive spectrum of a cuboidal inclusion showing the titanium-rich phase.

of the Fe-Ni phase diagram during the multipass welding led to the microsegregation of titanium and nickel at the HAZ II/parent metal interface.

2. This resulted in the formation of TiC/Ti(CN) particles and stable austenitic films on the grain boundaries.

3. Under the thermal stresses generated during

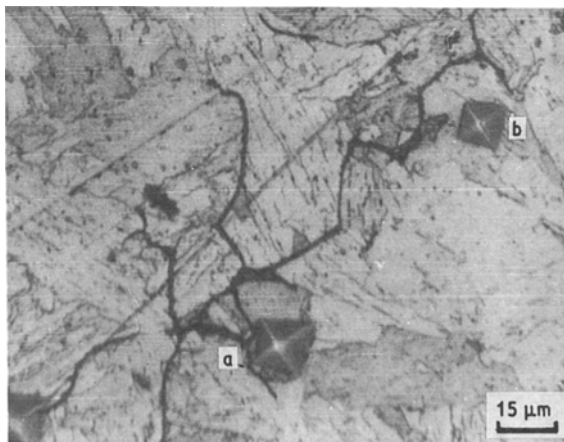


Figure 8 Micrograph showing microhardness indentation (a) near the grain boundaries having austenitic film and (b) in the martensitic matrix.

welding, microvoids were nucleated at the interfaces of TiC/Ti(CN) particles and austenite.

4. These microvoids were further propagated by microvoid coalescence due to the premature failure of austenitic film on grain boundaries.

### Acknowledgements

The authors thank Mr M. J. Nair, Head, MPD, Dr T. S. Lakshmanan, Head, MTESD, Dr K. V. Nagarajan, Group Head, MMG and Mr D. Easwar Das, Deputy

TABLE II EDAX analysis of different regions identified in Fig. 4

| Regions analysed (Fig. 4) | Alloying elements (wt %) |      |      |      |      |            |
|---------------------------|--------------------------|------|------|------|------|------------|
|                           | Ni                       | Co   | Mo   | Ti   | Al   | Balance Fe |
| A                         | 22.62                    | 6.79 | 7.11 | 0.60 | 0.11 | 62.77      |
| B                         | 20.01                    | 7.50 | 6.80 | 0.61 | 0.12 | 64.96      |
| C                         | 20.19                    | 8.11 | 5.44 | 0.46 | 0.07 | 65.73      |
| D                         | 20.86                    | 6.97 | 5.97 | 0.49 | 0.09 | 65.63      |
| E                         | 21.78                    | 7.32 | 5.51 | 0.82 | 0.08 | 64.50      |
| F                         | 22.43                    | 6.53 | 6.38 | 0.49 | 0.32 | 63.86      |
| G                         | 19.47                    | 7.69 | 5.60 | 0.68 | 0.54 | 66.02      |
| H                         | 19.25                    | 6.86 | 5.95 | 0.55 | 0.18 | 65.39      |
| I                         | 18.02                    | 8.79 | 5.49 | 0.96 | 0.09 | 66.65      |

Director, MMS for their constant encouragement during the course of this investigation. Permission granted to publish this paper by the Director, VSSC, is also gratefully acknowledged.

### References

1. J. J. PEPE and W. F. SAVAGE, *Weld. Res. Suppl.* **46** (1967) 411-s.
2. *Idem, ibid.* **49** (1970) 545-s.
3. NORMAN KEYNON, *ibid.* **47** (1968). 193-s.
4. W. R. ALBERT and W. S. PELLINI, *Weld. J. Res. Suppl.* **33** (1954) 835-s.
5. W. S. SAVAGE and C. D. LUNDIN, *ibid.* **44** (1965) 835-s.
6. A. M. HALL and C. J. SLUNDER, "The metallurgy, behaviour and applications of 18% Ni maraging steel", NASA, SP-5051 (1968).
7. A. GOLDBERG, *Weld. J. Res. Suppl.* **47** (5) (1968) 199.
8. T. BONISZEWSKI and K. BONISZEWSKI, *JISI* **204** (1966) 360.
9. J. A. PSIODA, PhD thesis, Carnegie Mellon University (1977).
10. A. S. TETLEMAN, Stanford University, Department of Materials Science, Report No 66-37 (1966).

*Received 27 April  
and accepted 29 November 1989*